Applied Physics Express

The Japan Society of Applied Physics

LETTERS • OPEN ACCESS

Significant photoresponsivity enhancement of polycrystalline $BaSi_2$ films formed on heated Si(111) substrates by sputtering

To cite this article: Satoshi Matsuno *et al* 2018 *Appl. Phys. Express* **11** 071401

View the article online for updates and enhancements.

Related content

- Exploring the potential of semiconducting BaSi2 for thin-film solar cell applications
Takashi Suemasu and Noritaka Usami
- Characterization of defect levels in undoped n-$BaSi_2$ epitaxial films on Si(111) by deep-level transient spectroscopy
Hiroki Takeuchi, Weijie Du, Masakazu Baba et al.
- p-$BaSi_2$/n-Si heterojunction solar cells on Si(001) with conversion efficiency approaching 10%: comparison with Si(111)
Tianguo Deng, Takuma Sato, Zhihao Xu et al.

This content was downloaded from IP address 130.158.56.100 on 19/07/2018 at 01:34

OPEN ACCESS

Applied Physics Express **11**, 071401 (2018)

https://doi.org/10.7567/APEX.11.071401

Significant photoresponsivity enhancement of polycrystalline $BaSi_2$ films formed on heated Si(111) substrates by sputtering

Satoshi Matsuno[1], Ryota Takabe[1], Seiya Yokoyama[1], Kaoru Toko[1], Masami Mesuda[2], Hideto Kuramochi[2], and Takashi Suemasu[1]

[1]*Institute of Applied Physics, University of Tsukuba, Tsukuba, Ibaraki 305-8573, Japan*
[2]*Tosoh Corporation, Advanced Materials Research Laboratory, Ayase, Kanagawa 252-1123, Japan*

Received May 2, 2018; accepted May 18, 2018; published online June 4, 2018

We fabricated approximately 200-nm-thick $BaSi_2$ films on Si(111) substrates at 600 °C. The formation of $BaSi_2$ was demonstrated by X-ray diffraction and Raman spectroscopy. A reduction in the electron concentration ($n = 2 \times 10^{16}\,cm^{-3}$) by 3 orders of magnitude compared to that previously reported ($n = 7 \times 10^{19}\,cm^{-3}$) and resultant photoresponsivity enhancement by more than two orders of magnitude were achieved. The photoresponsivity increased with the bias voltage V_{bias} applied between the top and bottom electrodes, and reached approximately 0.19 A/W at 2.0 eV, room temperature, and $|V_{bias}| = 0.5$ V. © 2018 The Japan Society of Applied Physics

Photovoltaic solar cell materials have been extensively studied over the past years.[1] Among them, we focused on the semiconducting barium disilicide ($BaSi_2$). Solar cell materials should be safe, stable, and earth-abundant, as Si. In addition, a solar cell material should have a large absorption coefficient (α), suitable band gap, and superior minority-carrier properties to achieve a high conversion efficiency (η). $BaSi_2$ has all of these properties[2,3] including a band gap of 1.3 eV,[4] large α of $3 \times 10^4\,cm^{-1}$ at 1.5 eV,[4–7] inactive grain boundaries,[8] and large minority-carrier lifetime ($\tau \sim 10$ μs).[9,10] We have achieved η approaching 10% in p-$BaSi_2$/n-Si heterojunction solar cells[11–13] and recently demonstrated the operation of $BaSi_2$ homojunction solar cells.[14] Extensive studies have been performed on $BaSi_2$ epitaxial films grown by molecular beam epitaxy (MBE). However, MBE is not a practical method to fabricate large-area solar cells. In contrast, vacuum evaporation is a more feasible method than MBE. An ultrahigh vacuum (UHV) is not a prerequisite; therefore, the equipment can be simple and inexpensive. Usami and Hara et al. used $BaSi_2$ granules to form $BaSi_2$ films by vacuum evaporation,[15–18] and achieved a high carrier lifetime of 4.8 μs in the films grown at 500 °C.[17] Another large-area thin-film growth technique is sputtering. Sputtering has been used to form semiconducting silicides such as β-$FeSi_2$ and Mg_2Si.[19,20] However, a limited number of studies have been reported on the formation of $BaSi_2$ films by sputtering.[21–23] Yang et al. formed polycrystalline $BaSi_2$ films on Si(111) by sputtering a Ba target at room temperature (RT), followed by post-annealings at temperatures in the range of 400 to 800 °C in an UHV.[21] The grown films contained metallic phases such as Ba_2Si and Ba_5Si_3. Instead of a Ba target, we employed a $BaSi_2$ sputtering target with a diameter of 2 in. and fabricated 600-nm-thick $BaSi_2$ films by radio-frequency (RF) magnetron sputtering at RT and subsequent post-annealing at 600 °C in an UHV. However, the photoresponsivity of the $BaSi_2$ film was as small as 0.5 mA/W at 1.5 eV at RT when the bias voltage was 0.5 V,[22] corresponding to an external quantum efficiency (*EQE*) of approximately 0.08%. The grown layer exhibited n-type conductivity with a large electron concentration of $n = 7 \times 10^{19}\,cm^{-3}$ at RT.

In this study, we used helicon-wave excited plasma (HWP) sputtering with a $BaSi_2$ target. As the HWP has a higher plasma density, uniform in a large volume,[24] and lower ion energy than those of usual capacitive-coupled plasmas, substrate damage can be reduced by this method. First, we investigated the dependences of the Ba-to-Si atomic ratios of the sputtered films at RT on the pressure (P) during the sputtering. We then attempted to form polycrystalline $BaSi_2$ films directly on a Si(111) substrate heated at 600 °C. The photoresponsivity was significantly improved by more than 2 orders of magnitude compared to those reported previously.[22]

Table I. Parameters of the sample preparation; the substrate, pressure (P) and substrate temperature (T_S) during the sputtering, layer thickness (d), and number of plate-like Ba sources on the target (N) are specified.

Sample	Substrate	P (Pa)	T_S (°C)	d (nm)	Rate (nm/min)	N
A1	CaF_2	0.25	RT	200	6.7	0
A2	CaF_2	1.0	RT	200	3.8	0
A3	CaF_2	3.0	RT	200	1.9	0
B1	Si(111)	0.25	RT	200	6.7	1
B2	Si(111)	1.0	RT	200	3.8	1
B3	Si(111)	3.0	RT	200	1.9	1
C	Si(111)	0.25	600	200	—	2
D1	Si(111)	0.25	600	220	—	3
D2	Si(111)	0.4	600	120	—	3

A polycrystalline stoichiometric $BaSi_2$ target (Tosoh) was used. Details of the sample preparation are summarized in Table I. As the distance between the target and substrate in the HWP sputtering system (ULVAC MB00-1014) is as long as approximately 20 cm, and the atomic weights of Ba and Si are significantly different, first, we investigated the Ba-to-Si atomic ratios of the sputtered films at RT. The flow rate of Ar was set to 10 sccm, the RF power was set to 100 W, while the P was varied in the range of 0.25 to 3.0 Pa during the sputtering. After the sputtering of $BaSi_2$, the samples were covered with a 20-nm-thick Al layer to prevent oxidation. The atomic ratio was measured by Rutherford backscattering (RBS) spectrometry, where the incident He-ion energy was set to 1.6 MeV; the backscattered ions with a scattering angle of 150° were detected. As described below, the obtained Ba atomic ratio corresponded to a deficient stoichiometry of the deposited films without an additional plate-like Ba source.

Content from this work may be used under the terms of the Creative Commons Attribution 4.0 license. Any further distribution of this work must maintain attribution to the author(s) and the title of the work, journal citation and DOI.

© 2018 The Japan Society of Applied Physics

Therefore, one, two, or three small pieces of plate-like Ba ($1.0 \times 1.0\,cm^2$) were added on the $BaSi_2$ target. The obtained samples are denoted as samples A, B, C, and D, respectively. We then attempted to form $BaSi_2$ films (samples C and D) at a heated Si(111) substrate at 600 °C, followed by capping with an approximately 3-nm-thick amorphous Si (a-Si) layer to prevent oxidation of the sample surface.[25] The crystalline qualities of the grown layers were characterized using grazing-incidence (GI) 2θ X-ray diffraction (XRD) with Cu-Kα radiation (Rigaku SmartLab) and Raman spectroscopy (JASCO NRS-5100) using a frequency-doubled neodymium-doped-yttrium–aluminum–garnet (Nd:YAG) laser (532 nm, 5.1 mW). For electrical characterizations of the sputtered films, we used a high-resistivity (ρ) p-type Si(111) ($\rho > 10^3$ Ωcm). Al electrodes were fabricated on the surface by RF sputtering. The carrier type and carrier concentration were characterized by Hall measurements using the van der Pauw method. For the photoresponsivity measurement, we used n^+-type Si(111) ($\rho < 0.01\,\Omega$cm) substrates. The low-ρ substrates provide a negligible contribution of photogenerated carriers in the n^+-Si substrate in the photoresponse measurement. Indium–tin oxide (ITO) surface electrodes with thicknesses of 80 nm and diameter of 1 mm and Al rear electrodes were fabricated by RF sputtering. The photoresponse spectra were acquired by a lock-in technique using a xenon lamp with a single monochromator with a focal length of 25 cm (Bunko Keiki SM-1700A and RU-60N). The light intensity of the lamp was calibrated using a pyroelectric sensor (Melles Griot 13PEM001/J).

As shown in Figs. 1(a) and 1(b), the atomic ratios of Ba and Si, and deposition rates of the sputtered films in the samples A1–A3 and B1–B3 depended on P, owing to the significantly different atomic weights of Si, Ar, and Ba, of 28.08, 39.95, and 137.33, respectively. In Fig. 1(a), the dotted and solid lines represent the results of the samples sputtered without and with one plate-like Ba source on the $BaSi_2$ target, respectively. The Si atomic ratio of the film (black dotted line) sputtered at $P = 0.25$ Pa was larger than 85%, and gradually decreased with the increase of P. However, it was still larger than 66.7% even at $P = 3.0$ Pa. In the formation of $BaSi_2$ films on a heated Si substrate, diffusion of Si atoms from the Si substrate occurs.[26] Therefore, the Si atomic ratio should be smaller than 66.7% at a given P to form $BaSi_2$ directly on a heated Si substrate. As shown by the black solid line in Fig. 1(a), the Si atomic ratio reached values below 66.7% at $P > 2.5$ Pa, which implies that the introduction of Ba pieces on the target is efficient to increase the Ba atomic ratio of the sputtered film. However, as shown in Fig. 1(b), the deposition rate of the film significantly decreased at $P > 2.5$ Pa. Based on these results, we considered that both high deposition rate and reduced Si atomic ratio below 66.7% would be simultaneously satisfied even at $P = 0.25$ Pa by adding two or more Ba sources on the $BaSi_2$ target.

Figure 2 shows GI-XRD patterns of the samples C and D1, with films sputtered at 600 °C and $P = 0.25$ Pa. For reference, the calculated diffraction pattern of the orthorhombic $BaSi_2$ is also shown. Although the diffraction patterns of the samples C and D1 slightly differed, all of the observed diffraction peaks were assigned to $BaSi_2$. Figure 3 shows the Raman spectrum of the sample D1. Similar Raman spectra were obtained for the samples C and D2. The Raman lines originated from Si tetrahedra with T_h symmetry in the lattice of $BaSi_2$. Identification of Raman lines is presented in Ref. 27. The transverse optical phonon line of Si (Si_{TO}) was observed even in such a thick $BaSi_2$ film. Considering that the absorption coefficient of $BaSi_2$ at a wavelength of 532 nm is $\alpha = 3 \times 10^5\,cm^{-1}$,[6] the penetration depth of the laser light was limited to around $1/\alpha \times 3 \sim 0.1\,\mu m$, hence the Si_{TO} signal is considered to originate from crystalline Si precipitates in the $BaSi_2$ film. Similar Si_{TO} signals were detected in $BaSi_2$[26,27] and β-$FeSi_2$ films[28] by Raman spectroscopy, which implies that excess Si atoms existed in the form of crystalline Si. The growth rate of $BaSi_2$ was approximately

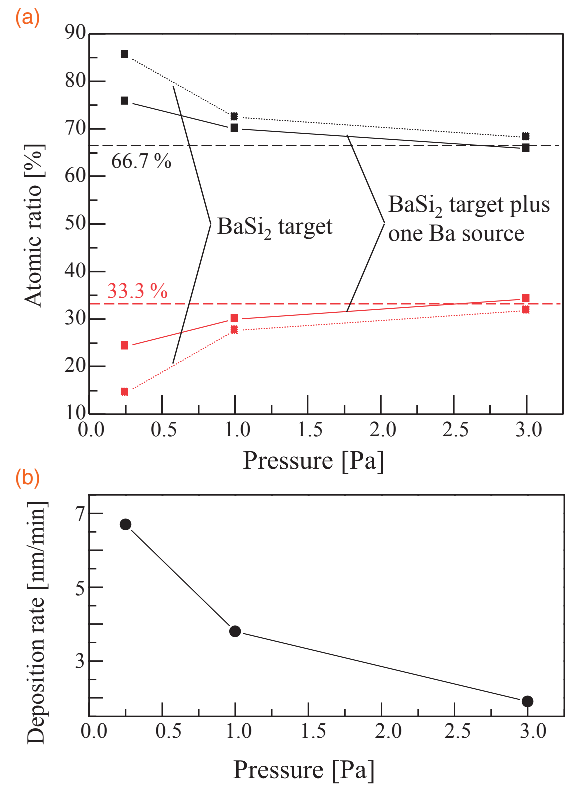

Fig. 1. Ba (red) and Si (black) atomic ratios as a function of P for the samples A1–A3 prepared without an additional Ba source (dotted lines) and B1–B3 with one Ba source on the $BaSi_2$ target (solid lines). The broken lines are plotted as guides showing the Ba and Si atomic ratios of the $BaSi_2$ target.

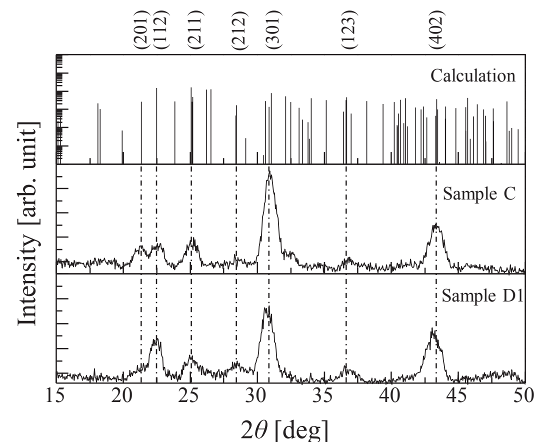

Fig. 2. GI-XRD patterns of the samples C and D1 sputtered at 600 °C on Si(111) substrates.

© 2018 The Japan Society of Applied Physics

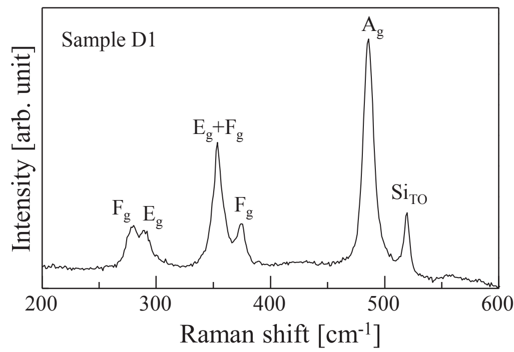

Fig. 3. Raman spectrum of the sample D1, with a film formed at 600 °C.

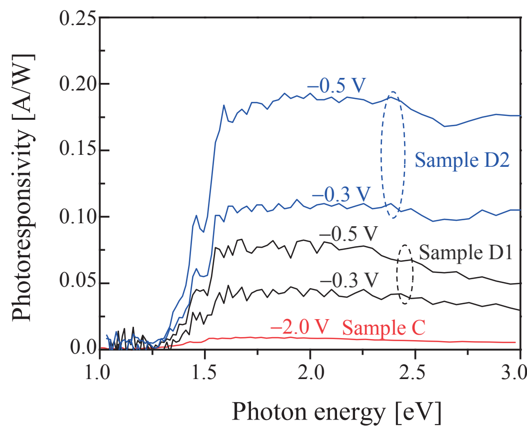

Fig. 4. Photoresponse spectra of the samples C, D1, and D2 measured at RT under various values of V_{bias} applied to the ITO electrode with respect to the Al electrode.

0.4 μm/h at $P = 0.25$ Pa, which is approximately four times higher than that by MBE.

Figure 4 shows the photoresponse spectra of the samples C, D1, and D2. The bias voltage (V_{bias}) was applied to the front ITO electrode with respect to the Al electrode to extract the photogenerated holes in n-$BaSi_2$ into the ITO electrode. The photoresponsivities of the samples D1 and D2 rapidly increased with V_{bias} for photon energies larger than the band gap of $BaSi_2$ (~1.3 eV), and reached 0.08 A/W and 0.19 A/W at 2.0 eV and $V_{bias} = -0.5$ V, corresponding to *EQE*s of 16 and 38%, respectively. These values are more than two orders of magnitude higher than those reported previously.[22] This improvement in photoresponsivity is attributed to the significant reduction in carrier concentration of the film. The electron concentrations of $BaSi_2$ in the samples D1 and D2 were approximately 2×10^{16} cm^{-3} at RT, obtained by a Hall measurement. This value is more than three orders of magnitude smaller than that previously reported ($n = 7 \times 10^{19}$ cm^{-3}).[22] In contrast, the photoresponsivity of the sample C was limited to approximately 0.01 A/W even at a higher V_{bias}. In addition, it was challenging to perform reliable Hall measurements of the $BaSi_2$ film of the sample C, indicating that the electrical and photoresponse properties are sensitive to the atomic ratio between Ba and Si. Similar results were obtained for $BaSi_2$ films grown by MBE.[26] Kumar et al.,[29] employing a supercell approach based on first-principle density functional theory, revealed that the formation energies of point defects in $BaSi_2$ such as Si vacancies, Ba anti-sites, and interstitial Si are dependent on the growth conditions, and that Si vacancies are most likely to emerge in $BaSi_2$ even in a Si-rich condition, yielding electrons. Therefore, the photoresponsivity can be increased significantly more by adjusting the Ba/Si atomic ratio and *P*. These results reveal that sputtering is a promising fabrication method for $BaSi_2$ films.

In summary, polycrystalline $BaSi_2$ films were directly formed by HWP sputtering at 600 °C. A typical value of $n = 2 \times 10^{16}$ cm^{-3} was obtained at RT by the van der Pauw method. The photoresponsivity rapidly increased for photon energies larger than the band gap of $BaSi_2$, and reached 0.19 A/W at 2.0 eV and $V_{bias} = -0.5$ V applied to the ITO electrode with respect to the Al electrode. This value was larger by more than two orders of magnitude from that reported previously.

Acknowledgments This study was financially supported by JSPS KAKENHI Grant Numbers 17K18865 and 18H03767 and JST MIRAI. R.T. was financially supported by a Grant-in-Aid for JSPS Fellows (15J02139).

1) M. A. Green, Prog. Photovoltaics **17**, 183 (2009).
2) J. Evers, G. Oehlinger, and A. Weiss, Angew. Chem., Int. Ed. **16**, 659 (1977).
3) M. Imai and T. Hirano, J. Alloys Compd. **224**, 111 (1995).
4) K. Morita, Y. Inomata, and T. Suemasu, Thin Solid Films **508**, 363 (2006).
5) D. B. Migas, V. L. Shaposhnikov, and V. E. Borisenko, Phys. Status Solidi B **244**, 2611 (2007).
6) K. Toh, T. Saito, and T. Suemasu, Jpn. J. Appl. Phys. **50**, 068001 (2011).
7) M. Kumar, N. Umezawa, and M. Imai, Appl. Phys. Express **7**, 071203 (2014).
8) M. Baba, M. Kohyama, and T. Suemasu, J. Appl. Phys. **120**, 085311 (2016).
9) K. O. Hara, N. Usami, K. Toh, M. Baba, K. Toko, and T. Suemasu, J. Appl. Phys. **112**, 083108 (2012).
10) K. O. Hara, N. Usami, K. Nakamura, R. Takabe, M. Baba, K. Toko, and T. Suemasu, Appl. Phys. Express **6**, 112302 (2013).
11) D. Tsukahara, S. Yachi, H. Takeuchi, R. Takabe, W. Du, M. Baba, Y. Li, K. Toko, N. Usami, and T. Suemasu, Appl. Phys. Lett. **108**, 152101 (2016).
12) S. Yachi, R. Takabe, K. Toko, and T. Suemasu, Appl. Phys. Lett. **109**, 072103 (2016).
13) T. Deng, T. Sato, Z. Xu, R. Takabe, S. Yachi, Y. Yamashita, K. Toko, and T. Suemasu, to be published in Appl. Phys. Express.
14) K. Kodama, K. Toko, and T. Suemasu, Jpn. J. Appl. Phys. **57**, 050310 (2018).
15) K. O. Hara, Y. Nakagawa, T. Suemasu, and N. Usami, J. Appl. Phys. **54**, 07JE02 (2015).
16) K. O. Hara, C. T. Trinh, K. Arimoto, J. Yamanaka, K. Nakagawa, Y. Kurokawa, T. Suemasu, and N. Usami, J. Appl. Phys. **120**, 045103 (2016).
17) C. T. Trinh, Y. Nakagawa, K. O. Hara, R. Takabe, T. Suemasu, and N. Usami, Mater. Res. Express **3**, 076204 (2016).
18) T. Suhara, K. Murata, A. Navabi, K. O. Hara, Y. Nakagawa, C. T. Trinh, Y. Kurokawa, T. Suemasu, K. L. Wang, and N. Usami, Jpn. J. Appl. Phys. **56**, 05DB05 (2017).
19) T. Yoshitake, A. Yuri, and K. Nagayama, Appl. Phys. Lett. **88**, 182104 (2006).
20) S. Ogawa, A. Katagiri, T. Shimizu, M. Matsushima, K. Akiyama, Y. Kimura, H. Uchida, and H. Funakubo, J. Electron. Mater. **43**, 2269 (2014).
21) Z. Yang, Z. Hao, and Q. Xie, Phys. Procedia **11**, 118 (2011).
22) T. Yoneyama, A. Okada, M. Suzuno, T. Shibutam, K. Matsumaru, N. Saito, N. Yoshizawa, K. Toko, and T. Suemasu, Thin Solid Films **534**, 116 (2013).
23) N. A. A. Latiff, T. Yoneyama, T. Shibutami, K. Matsumaru, K. Toko, and T. Suemasu, Phys. Status Solidi C **10**, 1759 (2013).
24) K. Yamaya, Y. Yamaki, H. Nakanishi, and S. Chichibu, Appl. Phys. Lett. **72**, 235 (1998).
25) R. Takabe, W. Du, K. Ito, H. Takeuchi, K. Toko, S. Ueda, A. Kimura, and T. Suemasu, J. Appl. Phys. **119**, 025306 (2016).
26) R. Takabe, T. Deng, K. Kodama, Y. Yamashita, T. Sato, K. Toko, and T. Suemasu, J. Appl. Phys. **123**, 045703 (2018).
27) Y. Terai, H. Yamaguchi, H. Tsukamoto, N. Murakoso, M. Iinuma, and T. Suemasu, Jpn. J. Appl. Phys. **56**, 05DD02 (2017).
28) M. Iinuma, H. Tsukamoto, N. Murakoso, H. Yamaguchi, and Y. Terai, JJAP Conf. Proc. **5**, 011106 (2017).
29) M. Kumar, N. Umezawa, W. Zhou, and M. Imai, J. Mater. Chem. A **5**, 25293 (2017).

© 2018 The Japan Society of Applied Physics